High-resolution Compton line shapes: Fermi break of beryllium

S. Huotari,[1] C. Sternemann,[2] M. Volmer,[2] J. A. Soininen,[3] G. Monaco,[1] and W. Schülke[2]
[1]*European Synchrotron Radiation Facility, Boîte Postale 220, F-38043 Grenoble Cedex, France*
[2]*Fakultät Physik/DELTA, Technische Universität Dortmund, D-44221 Dortmund, Germany*
[3]*Division of X-ray Physics, Department of Physical Sciences, P. O. Box 64, FIN-00014 University of Helsinki, Finland*
(Received 28 August 2007; published 6 December 2007; corrected 12 December 2007)

The Be[110] Compton profile was measured with high resolution utilizing x rays with energy of 16–18 keV. The momentum resolution due to the experimental factors was set to 0.018 atomic units of momentum (a.u.). Electron final-state effects were estimated to have an approximate broadening effect of the spectral features equivalent to 0.028 a.u., resulting in a total momentum resolution of 0.033 a.u., i.e., more than a factor of 2 better than in previous Compton scattering studies. In this way, it was possible to study the ground-state momentum density of the electrons in metallic beryllium with a very high accuracy. As a result, the Fermi-surface-related fine structure is well observed in the experimental Compton profile and its derivative. However, the observed features are broader and less pronounced than anticipated by theoretical estimates. The remaining difference may be due to a non-negligible ground-state correlation and its effects on the momentum density and the Fermi surface of beryllium metal.

DOI: 10.1103/PhysRevB.76.235106 PACS number(s): 71.18.+y, 71.10.Ca, 71.20.Gj, 07.85.Qe

I. INTRODUCTION

Compton scattering is a widely used tool to study the ground-state properties of electrons in solids and molecular systems.[1,2] For example, this technique can be used to obtain information on the Fermi surface of metals, by either Fermi surface reconstruction using directional Compton profiles[3–7] or direct observation of Fermi-surface-related signatures in the Compton profile.[8–11] In an inelastic x-ray scattering experiment, the measured quantity is the double-differential cross section

$$\frac{d^2\sigma}{d\omega\, d\Omega} = \left(\frac{d\sigma}{d\Omega}\right)_{\mathrm{Th}} \frac{\omega_2}{\omega_1} S(\mathbf{q},\omega), \tag{1}$$

where ω and $\mathbf{q}$ are the energy and momentum transfers, respectively, $(d\sigma/d\Omega)_{\mathrm{Th}}$ is the Thomson cross section, ω_1 and ω_2 are the incident and scattered photon energies, respectively, and $S(\mathbf{q},\omega)$ is the dynamic structure factor. Within the so-called impulse approximation[12] (IA) $S(\mathbf{q},\omega)$ reduces to the Compton profile $J(p_z)$,

$$S^{\mathrm{IA}}(\mathbf{q},\omega) = J(p_z)/q, \tag{2}$$

where $p_z=(\omega-q^2/2)/q$ is the projection of the momentum vector of the electron participating in the scattering process along $\mathbf{q}$. We adopt here atomic units with $e=m=\hbar=1$. The Compton profile is directly related to the ground-state momentum density $N(\mathbf{p})$ of the electrons and it can be expressed as its average over two dimensions,

$$J(p_z) = \int_{-\infty}^{\infty}\int_{-\infty}^{\infty} N(\mathbf{p})\, dp_x dp_y. \tag{3}$$

In the case of metals, the shape of the momentum density near the Fermi surface is of fundamental interest to solid-state physics. The most commonly used methods to study the Fermi-surface-related features are photoemission spectroscopy, positron annihilation, de Haas–van Alphen measurements, and Compton scattering. The advantage of Compton scattering is that it is bulk sensitive and does not require special conditions for the sample environment. The disadvantage, however, has been the relatively poor resolution and low signal, resulting in lengthy measurements. De Haas–van Alphen measurements require a combination of a long electronic mean free path and high magnetic fields, and are usually performed at $T \lesssim 100$ K.[13] Momentum-resolved photoemission spectroscopy can be used mostly for surface studies but offers a very good momentum and spatial resolution. Positron annihilation spectroscopy is sensitive to defects, but this does not normally pose problems in studies of the Fermi surface in a large variety of systems. Perhaps most importantly, it offers the possibility of studying higher-Z elements and compounds than is usually possible with high-resolution Compton scattering.[14] However, the presence of the positron wave function gives raise to electron-positron correlation, modifying the measured Fermi function in a way that makes studies of electron-electron correlation difficult.[15] Another reason to use positron annihilation and Compton scattering is that they provide information not only on the Fermi surface, but also on the high-momentum (umklapp) components of the electron wave functions in solids.[16,17]

The result of all the latest high-resolution Compton scattering experiments on metals like Be and Li has been that the presumably sharp Fermi-surface-related structures in the Compton profiles of metals seem to be much broader than expected.[11,18–20] Experiments[11,21] that attempted to probe the momentum density of Be metal with a momentum resolution of the order of 0.02 a.u. found this broadening especially severe. It was pointed out that, in order to fully describe the Compton line shape as observed in those experiments, the final state of the scattering electron has also to be taken into account. This was done by introducing the spectral density function (SDF) of the final-state electron $A(\mathbf{k},\epsilon)$, where $\mathbf{k}$ and ϵ are the momentum and energy of the electron, respectively. This was done for the first time in the *GW* approximation,[20,22] and later in an approximation that allowed the SDF to be written analytically.[23]

Within the limits of the IA, the final electron state is assumed to be a plane wave and its SDF a Dirac δ function. In reality this is never exactly the case, and this effect can be approximately included by expressing the dynamic structure factor as[23]

$$S(\mathbf{q},\omega) = \int S^{\mathrm{IA}}(\mathbf{q},\epsilon)\tilde{A}(\mathbf{q},\omega-\epsilon)d\epsilon, \tag{4}$$

where $\tilde{A}(\mathbf{q},\epsilon)=A(\mathbf{q},\epsilon+q^2/2)$ (see Ref. 23 for details).

Experiments that aspired to achieve the best possible resolution used photon energies of ~10 keV, and the energy transferred to the valence electrons was typically 400 eV. In order to make the IA applicable, the energy and momentum transferred to the electron should be large in comparison with its initial energy and momentum (e.g., the binding energy of core electrons, or the Fermi energy of valence electrons).[12] It was expected that, since the energy transfer was large in comparison to the Fermi energy of Be (14.3 eV), the IA should be valid for the valence electrons. It is now understood that it was not the case, since the lifetime width of the SDF vanishes relatively slowly as a function of momentum and energy transfer. This means that experiments performed around 10 keV are not probing the ground-state momentum density as expected. This is unfortunate, since in principle the current design of spectrometers for such energies would allow the best momentum resolution in Compton-scattering experiments. For example, the resolution in terms of electron momentum mapping of a backscattering spectrometer operating at less than 20 keV would be easily achieved to be below 0.02 a.u., whereas the spectrometers designed for energies above 30 keV have a resolution of 0.1 a.u. at best.[24–26]

For these reasons, the separation between the ground-state correlation and the final-state effects in the Fermi-structure-related information is a demanding task. However, gaining true access to the ground-state correlations would give a very fundamental verification for modern solid-state theories. Based on the results of several previous studies,[11,18,21] one of the best candidates for accessing the problem in the Compton-scattering regime is the Be[110] Compton profile, due to its Fermi-surface-related fine structure and observed differences between experiment and theory. This kind of study is possible only if the final-state effects of Compton scattering are minimized while gaining the highest possible momentum space resolution.

The Fermi surface of beryllium has been studied with many different methods.[27–30] In the empty-lattice model the four electrons per unit cell fill the first two Brillouin zones. The electron-ion interaction causes a coronet-shaped volume of holes in the second zone, the corresponding electrons being shifted to the third zone, forming a cigarlike structure perpendicular to the basal plane. Its projection on this plane is centered around the K point at a distance 0.97 a.u. from the origin Γ. These structures will give small but interesting modulations to the Compton profiles. In particular, the profile along [110] exhibits the following features, depicted in Fig. 1. First of all, the shape of the Compton profile follows roughly the shape of the first Brillouin zone. As one traverses

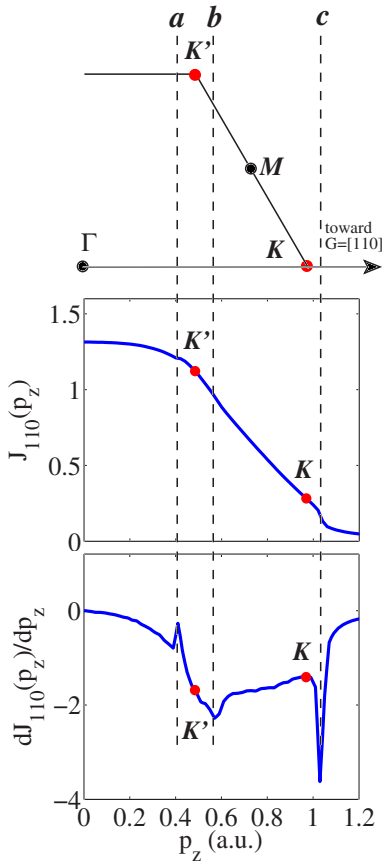

FIG. 1. (Color online) Top panel: Basal plane of the first Brillouin zone. Middle and bottom panels: Theoretical Compton profile along the [110] direction as calculated by Bansil and Kaprzyk (Ref. 11), and its derivative. The features labeled *a*, *b*, and *c* and marked with vertical dashed lines point to Fermi-surface-related features discussed in the text.

along the first Brillouin zone from Γ toward the corner K before the K' point enters into the integration plane, the area of the slice of the first Brillouin zone is independent of p_z, making the Compton profile very flat. After that the area of the Brillouin zone slice and consequently also the Compton profile decrease linearly until K. The fine structure, on the other hand, can be understood in terms of the coronet and cigar structures. Just before K', at around 0.40 a.u., the first surfaces of the cigars centered around the K' points are traversed and there is a small jump in the momentum density because of this (labeled *a* in Fig. 1). These two cigars end at around 0.55 a.u., causing a dip in the Compton profile derivative (label *b*), broadened by the coronet structure. The beginning of the cigar at the last K point does not cause a large jump in the derivative, probably also due to a broadening effect of the coronet. The end of the cigar will cause a drop in the Compton profile, clearly visible in its derivative (label *c*) and marking the end of the Fermi surface. The position of this drop will give an estimate of the size of the cigar in the ΓK direction since it is known that it is centered at K, i.e., $\left[\frac{1}{3}\frac{1}{3}0\right]$ at 0.97 a.u. However, after extensive searches of this Fermi-surface structure in the Be[110] Compton profiles,[9,11,21] it has been never well resolved before. Only Itou *et al.*[9] have observed this feature, but any

detailed study would require higher momentum resolution than has been available previously. As this cigar-related structure has always been found to be weaker in the experimental results than predicted by theoretical estimates, it has been suggested that perhaps the structure is smeared out by large ground-state electron-electron correlations. Since the finite experimental resolution and possibly large final-state effects may also make it difficult to observe the feature, the existence of these sharp structures in the Compton profile is still under debate.

In this paper, we report an experimental high-resolution Compton profile of a Be single crystal with momentum transfer along the reciprocal lattice vector [110]. The aim was to study the ground-state electron momentum density of a simple metal. The prerequisite for such a measurement is to satisfy both requirements of very high momentum space resolution and a small contribution of final-state effects. We show that the Fermi-surface-related fine structure does indeed exist in the Be Compton profile and is not completely smeared out. Nevertheless, it is still found to be broader than expected, implying the possibility of relatively important ground-state correlation effects.

The paper is arranged as follows. In Sec. II the experimental details are discussed. Sec. III presents the results and discussion, and conclusions are drawn in Sec. IV.

II. EXPERIMENT

The aim of the experimental setup was to find an optimized compromise between maximizing momentum space resolution and minimizing final-state effects. This may be reached by using x rays with intermediate x-ray energies (in this case, 16–18 keV) instead of choosing very high x-ray energies (for example, 60–120 keV). Naturally this approach is limited to low-Z elements, but with current synchrotron radiation sources, studies at least up to Na ($Z=11$) are feasible with a momentum resolution of 0.02 a.u., and many interesting systems, including organic crystals, metals and semiconductors like Li, Na, Mg, Al, and Si, can be studied, if the contribution of the core electrons is taken into account properly.

The Compton profile of single-crystal Be with momentum transfer vector $\mathbf{q}$ along the [110] reciprocal lattice direction was measured at the beamline ID16 at the European Synchrotron Radiation Facility (Grenoble, France). The radiation from three consecutive undulators with a 35-mm period was monochromatized by a double-crystal fixed-exit Si(111) monochromator to energies between 15.8 and 17.8 keV. The beam size at the sample was 0.7 mm[vertical(V)] $\times$2.0 mm[horizontal(H)].

The spectrometer to analyze the scattered radiation consisted of a spherically bent Si(888) crystal, which operated in the Johann geometry with 1-m bending radius, and a Peltier-cooled Si solid-state detector. The Bragg angle was fixed to 89.7°, and the energy of the detected radiation was 15.817 keV. The scattering angle was $2\theta=158°$, resulting in a momentum transfer at the Compton peak of 8.6 a.u. The effectively used analyzer crystal area was 20 mm(H) $\times$100 mm(V), resulting in an uncertainty of the momentum transfer of 0.017 a.u. The bandwidth of the incident radiation varied between 1.8 and 2.0 eV in the energy range 15.8–17.8 keV, and the reflection bandwidth of the analyzer crystal was 2.0 eV. The p_z resolution (i.e., the electron-momentum resolution) was determined by calculating numerically the distribution of the scattering angles on the analyzer crystal.[31] The resolution function was found to have an approximately Gaussian shape with a full width at half maximum (FWHM) of 0.018 a.u.

The sample was a single crystal of Be with a cross section of 1.0×1.0 mm^2 and length of 8 mm. This sticklike sample was kept horizontally so that the polarization of the incident radiation was along the c axis. The contribution of multiple scattering was calculated by a Monte Carlo simulation[32] taking into account the sample geometry and the polarization of the photon field. The contribution of multiple scattering to the total scattering was estimated to be 2.2%, and had a negligible effect on the results presented in this paper. The energy scans were performed by tuning the Bragg angle of the double-crystal monochromator and the undulator gaps simultaneously. The count rate was about 1000 counts/s at the Compton profile peak. A total of 1.4×10^5 counts in the Compton profile peak were collected within a channel of 0.01 a.u. in momentum. The statistical error bar in the Compton peak was thus 0.26% of $J(0)$. However, the interesting Fermi-surface-related features are not located at the peak and thus the measurements were concentrated mostly at the Fermi edge around $p_z=1.0$ a.u.

Spectra were corrected for changes in the incident photon flux, sample self-absorption, and detector dead time, and finally transformed into momentum scale using the relativistic formulas of Holm.[33] Note that in this convention negative values of p_z correspond to large values of energy transfer. Finally, the experimental Compton profile was normalized to the same area as the theoretical Compton profile in the region $|p_z|<3.5$ a.u. and the IA-based core electron Compton profile was directly subtracted after the normalization.

III. RESULTS AND DISCUSSION

The experimental Compton profile is compared to a theoretical Compton profile computed within the IA- and local density approximation–(LDA) based band theory framework by Bansil and Kaprzyk, and presented previously in Ref. 11. The ground-state correlations are taken approximately into account by the use of the isotropic Lam-Platzman correction,[34] calculated by using the difference between the momentum density of an interacting and a noninteracting homogeneous electron system taken at the local density. The effect of the electron final state is taken into account using the SDF formalism of Ref. 23 and convoluting the valence-electron Compton profile in the energy scale with the calculated SDF according to Eq. (4). Figure 2 presents the SDF line shape in energy and momentum scales for two momentum transfer values corresponding to this and a previous[11] experiment. The SDF consists of a large quasiparticle peak and a small secondary quasiparticle-plasmon peak. The finite width of the SDF is due to the self-energy of the final-state electron. In this experiment, the Compton shift, classically

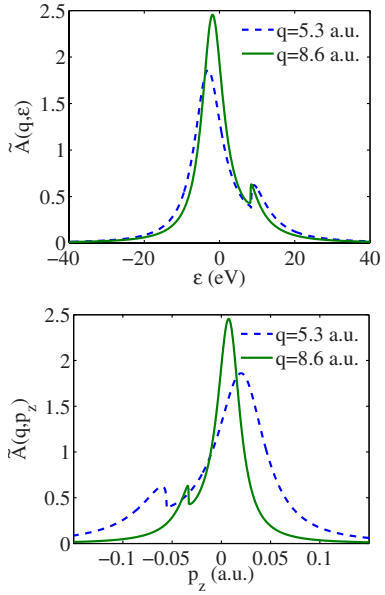

FIG. 2. (Color online) Spectral density function for a free-electron gas with the electron density of Be for two different momentum transfers. The dashed line corresponds to the experiment performed with 10-keV photons (Ref. 11) and the solid line to the present experiment. In the upper panel, the SDF is presented in the energy scale and in the lower panel as a function of p_z, i.e., on the final experimental scale.

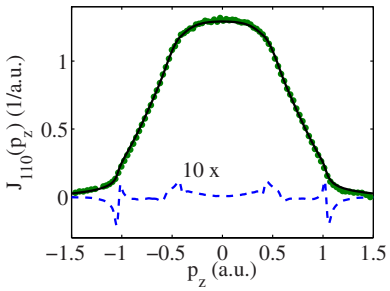

FIG. 3. (Color online) Solid line: theoretical Be[110] valence Compton profile from Fig. 1 with the correction due to final-state effects taken into account in the spectral density function formalism of Ref. 23. Dashed line: the difference of the latter and the impulse-approximation-based Compton profile magnified by ten for better visibility. Circles: the measured Be[110] valence Compton profile (only every third measured point is plotted for clarity). The statistical uncertainties of the experimental data points are smaller than the symbol size.

given by $q^2/2$, is 1.0 keV, i.e., larger than the 400 eV in previous experiments that attempted to achieve similar momentum space resolution.[11,21] However, the FWHM of the SDF in the energy space is only 23% smaller in this experiment than in the previous studies where 10-keV photons were utilized as the probe. Nevertheless, as pointed out in Ref. 23, the factor that matters more is the relationship between the photon energy and the corresponding scattering-electron momentum, and as the incident photon energy gets larger, the Compton profile gets broader in energy. As a result, while the SDF does not change greatly in energy space as a function of momentum transfer between 5.3 and 8.6 a.u., it narrows in p_z space by a substantial amount, which is clearly observed in the lower panel of Fig. 2. Therefore, a relatively small increase in the probing x-ray energy reduces the influence of the SDF significantly. The final momentum space resolution in the present experiment was found to be 0.028 a.u., due to final-state effects and 0.018 a.u. due to geometrical contributions, giving a total resolution of $\Delta p_z = 0.033$ a.u. The corresponding contributions in a previous experiment[11] were 0.061 a.u. due to final-state effects and 0.020 a.u. due to geometrical contributions, giving a total of 0.067 a.u. All these numbers refer to the total FWHM, taking into account in all cases the real shapes of the corresponding functions (close to Lorentzian for the SDF except for the small quasiparticle-plasmon peak, and close to Gaussian for the resolution function).

The Be[110] valence-electron Compton profile is presented in Fig. 3. Experimental data are compared to the LDA-based Compton profile after including the final-state effects via the SDF formalism. The experimental valence Compton profile is obtained by subtracting the LDA-based 1*s* profile (calculated within the IA). The effect of the SDF is depicted as the difference between the IA-based profile and the SDF-corrected one. The effect is especially seen at the Fermi-surface-related structures at the points K' and K (see Fig. 1). As mentioned in the Introduction and as can also be seen in Fig. 3, the Be[110] Compton profile is very flat up to $|p_z| = 0.4$ a.u., after which it decreases with almost a constant slope until 1.0 a.u., where the Fermi surface is crossed for the last time. An interesting feature between the calculated and the experimental Compton profile is that the Compton profile peak height at $p_z = 0$ is very close to the one predicted by the theory. In previous experiments performed with higher photon energies (30–60 keV) (regardless of the choice of the sample), the Compton profile peak height has always been found to be lower than theoretically predicted, and this has been partly assigned as an effect of correlation. However, the present experimental result is in agreement with previous experiments performed with 10-keV photons,[11] where no large discrepancy in the value of $J(0)$ was found. The exact value of $J(0)$ depends naturally on the normalization. Although the tails of the Compton profile of Be extend to about $|p_z| \sim 6$ a.u.,[9] in the present case the measurement could be done only within $|p_z| < 4$ a.u. due to the presence of the elastic line. Thus the experimental Compton profile was normalized to have the same area as the theoretical profile in the region $|p_z| < 3.5$ a.u. corresponding to 3.83 electrons. Due to the very good agreement between experimental and theoretical profiles, the value of $J(0)$ was found not to be sensitive to the normalization when its range was varied between $|p_z| < 1$ and 3.5 a.u.

The most interesting features can be observed when the data sets are compared through their derivatives. The derivatives of the data were taken using a three-point numerical derivative without smoothing, using the same point grid for both experimental and theoretical data sets. In particular, we turn our attention to certain Fermi-surface-related features around the Fermi momentum. Figure 4 presents the derivatives of the Compton profile concentrated on the region around $p_z = 1.0$ a.u. With the improved experimental accu-

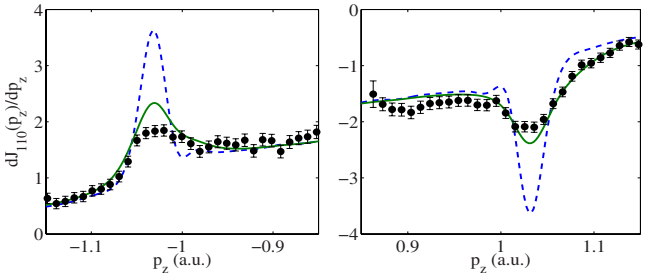

FIG. 4. (Color online) Fine structures of the Be[110] Compton profile derivatives. The dots with error bars refer to the experimental result and its statistical accuracy. The dashed line refers to the LDA calculation including the experimental resolution function, while the solid line includes also the final-state effects via an additional convolution of the dashed curve with the SDF. The Fermi-surface-caused peak (left) or dip (right) at $|p_z|=1.027$ a.u. is clearly visible in the experimental data but slightly broader than anticipated by the theoretical curve, suggesting the possibility of a non-negligible ground-state correlation.

racy of the present study, it is possible to observe the Fermi-surface-related dip (or peak in the negative momentum side) between $|p_z|=1.0$ and 1.1 a.u., which was not observed in previous studies using similar spectrometers due to their lower resolving power.[11,21] In the SDF-corrected theoretical profile the position of the SDF on the energy axis was determined so that the positions of the Fermi-surface-related structures in the Compton profile derivative remain symmetric with respect to $p_z=0$, a criterion that was used also in the analysis of the experimental data. As discussed in the Introduction (see Fig. 1), this peak marks the end of the cigar-related Fermi surface near the K point of the first Brillouin zone. It can be inferred from the experimental data that this point is at $p_z=1.027\pm0.005$ a.u., in excellent agreement with the theoretical result. It can be seen that this feature is still found to be broader in the experiment than predicted by the LDA-based theory even when the final-state effects are accounted for. This could be due to a relatively important ground-state correlation effect smearing the surface of the cigar, a result very often seen in many Compton-scattering studies. As pointed out by Barbiellini and Bansil,[35] this additional broadening of Fermi-surface related features can be accounted for in a Bardeen-Cooper-Schrieffer-like approach by constructing the many-body wave function as an antisymmetrized geminal product. While the theoretical Compton profile used in this study is calculated assuming the IA and reflects only the ground-state electron momentum density, the final-state effects in the scattering process are taken into account within the SDF formalism. However, this is by no means the only possible approach. For instance, Kaplan *et al.*[36] have considered taking the final-state effects into account implicitly by calculating the partial triply differential cross section. This approach relies on the simultaneous measurement of the ejected electron in coincidence with the scattered photon. While that was not within the scope of the present experiment, studies of that kind should give more insight into the role of final-state effects in Compton scattering. It should be emphasized that the width of the SDF grows with increasing electron density. Beryllium, being one of the highest-density elemental metals, has a very broad SDF. For most of the other metals the SDF width is much less important, and studies for the alkali metals, for instance, can be done with the presented experimental setup with much smaller final-state effects. The current study proves that very high-resolution Compton scattering studies are indeed possible with photon energies of the order of 15–18 keV for low-Z elements, and momentum resolution in such experiments can be pushed beyond 0.02 a.u. Studies of the Fermi structures of low-Z metals are thus possible using the proposed setup with very high resolution.

IV. CONCLUSIONS

The Compton profile of Be[110] was studied with inelastic x-ray scattering with intermediate photon energies of 16–18 keV. The spectrum of Compton-scattered photons was analyzed in terms of the ground-state momentum density, taking into account final-state effects in the scattering process. The momentum density was compared to computational Compton profiles based on calculations within the LDA. With the presented experimental setup, the influence of final-state effects was minimized while keeping the electron-momentum resolution as high as possible. The total effective resolution was $\Delta p_z=0.033$ a.u., out of which 0.028 a.u. was due to the spectral-density function of the final state and 0.018 a.u. due to the experimental resolution. With this improved sensitivity it was possible to probe the ground-state momentum density with a higher resolution than has been previously possible. The cigar-related Fermi surface and its position in the [110] (ΓK) direction was clearly observed in the experimental Compton profile. It was found, however, that the ground-state momentum density exhibits broadening not explained either by the LDA ground-state calculation or by the final-state effects. This result is in agreement with those of previous studies. The remaining discrepancy may be due to incomplete description of ground-state electron-electron correlation effects.

ACKNOWLEDGMENTS

We are grateful to R. Verbeni, G. Vankó, C. Henriquet, and T. Pylkkänen for help during the experiments and for critical discussions. A. Bansil and S. Kaprzyk are gratefully acknowledged for the permission to use their theoretical Compton profile. C.S. and M.V. would like to thank M. Tolan for his encouragement. Our gratitude also goes to T. Buslaps for lending the sample. J.A.S. is supported by the Academy of Finland (Contract No. 110571/1112642).

[1] *X-Ray Compton Scattering*, edited by M. Cooper (Oxford University Press, Oxford, 2004).
[2] W. Schülke, *Electron Dynamics by Inelastic X-Ray Scattering* (Oxford University Press, Oxford, 2007).
[3] N. Hiraoka, T. Buslaps, V. Honkimäki, J. Ahmad, and H. Uwe, Phys. Rev. B **75**, 121101(R) (2007).
[4] N. Hiraoka, T. Buslaps, V. Honkimäki, T. Nomura, M. Itou, Y. Sakurai, Z. Q. Mao, and Y. Maeno, Phys. Rev. B **74**, 100501(R) (2006).
[5] G. Kontrym-Sznajd, M. Samsel-Czekała, S. Huotari, K. Hämäläinen, and S. Manninen, Phys. Rev. B **68**, 155106 (2003).
[6] I. Matsumoto, H. Kawata, and N. Shiotani, Phys. Rev. B **64**, 195132 (2001).
[7] W. Schülke, G. Stutz, F. Wohlert, and A. Kaprolat, Phys. Rev. B **54**, 14381 (1996).
[8] Y. Sakurai, Y. Tanaka, A. Bansil, S. Kaprzyk, A. T. Stewart, Y. Nagashima, T. Hyodo, S. Nanao, H. Kawata, and N. Shiotani, Phys. Rev. Lett. **74**, 2252 (1995).
[9] M. Itou, Y. Sakurai, T. Ohata, A. Bansil, S. Kaprzyk, Y. Tanaka, H. Kawata, and N. Shiotani, J. Phys. Chem. Solids **59**, 99 (1998).
[10] C. Filippi and D. M. Ceperley, Phys. Rev. B **59**, 7907 (1999).
[11] S. Huotari, K. Hämäläinen, S. Manninen, S. Kaprzyk, A. Bansil, W. Caliebe, T. Buslaps, V. Honkimäki, and P. Suortti, Phys. Rev. B **62**, 7956 (2000).
[12] P. Eisenberger and P. M. Platzman, Phys. Rev. A **2**, 415 (1970).
[13] P. A. Goddard, J. Singleton, R. D. McDonald, N. Harrison, J. C. Lashley, H. Harima, and M.-T. Suzuki, Phys. Rev. Lett. **94**, 116401 (2005).
[14] Z. Major *et al.*, Phys. Rev. Lett. **92**, 107003 (2004).
[15] G. Kontrym-Sznajd and A. Rubaszek, Phys. Rev. B **47**, 6950 (1993).
[16] H. Sormann and M. Šob, Phys. Rev. B **41**, 10529 (1990).
[17] S. Huotari, K. Hämäläinen, S. Manninen, C. Sternemann, A. Kaprolat, W. Schülke, and T. Buslaps, Phys. Rev. B **66**, 085104 (2002).
[18] T. Ohata, M. Itou, I. Matsumoto, Y. Sakurai, H. Kawata, N. Shiotani, S. Kaprzyk, P. E. Mijnarends, and A. Bansil, Phys. Rev. B **62**, 16528 (2000).
[19] Y. Tanaka, Y. Sakurai, A. T. Stewart, N. Shiotani, P. E. Mijnarends, S. Kaprzyk, and A. Bansil, Phys. Rev. B **63**, 045120 (2001).
[20] C. Sternemann, K. Hämäläinen, A. Kaprolat, A. Soininen, G. Döring, C.-C. Kao, S. Manninen, and W. Schülke, Phys. Rev. B **62**, R7687 (2000).
[21] K. Hämäläinen, S. Manninen, C.-C. Kao, W. Caliebe, J. B. Hastings, A. Bansil, S. Kaprzyk, and P. M. Platzman, Phys. Rev. B **54**, 5453 (1996).
[22] L. Hedin, Phys. Rev. **139**, A796 (1965); the name of the *GW* approximation arises from the fact that the electron self-energy involves the product of the electron Green's function *G* and the dynamically screened Coulomb interaction *W*.
[23] J. A. Soininen, K. Hämäläinen, and S. Manninen, Phys. Rev. B **64**, 125116 (2001).
[24] P. Suortti *et al.*, J. Synchrotron Radiat. **6**, 69 (1999).
[25] N. Hiraoka, T. Buslaps, V. Honkimäki, and P. Suortti, J. Synchrotron Radiat. **12**, 670 (2005).
[26] N. Hiraoka, M. Itou, T. Ohata, M. Mizumaki, Y. Sakurai, and N. Sakai, J. Synchrotron Radiat. **8**, 26 (2001).
[27] T. L. Loucks and P. H. Cutler, Phys. Rev. **133**, A819 (1964).
[28] S. Chatterjee and P. Sinha, J. Phys. F: Met. Phys. **5**, 2089 (1975).
[29] D. A. Papaconstantopoulos, *Handbook of the Band Structure of Elemental Solids* (Plenum Press, New York, 1986).
[30] J. H. Tripp, W. L. Gordon, and P. M. Everett, Phys. Lett. **26**, 98 (1967).
[31] S. Huotari, K. Hämäläinen, S. Manninen, A. Issolah, and M. Marangolo, J. Phys. Chem. Solids **62**, 2205 (2001).
[32] P. Fajardo, V. Honkimäki, T. Buslaps, and P. Suortti, Nucl. Instrum. Methods Phys. Res. B **134**, 337 (1999).
[33] P. Holm, Phys. Rev. A **37**, 3706 (1988).
[34] L. Lam and P. M. Platzman, Phys. Rev. B **9**, 5122 (1974).
[35] B. Barbiellini and A. Bansil, J. Phys. Chem. Solids **62**, 2181 (2001).
[36] I. G. Kaplan, B. Barbiellini, and A. Bansil, Phys. Rev. B **68**, 235104 (2003).